Surface Analysis of Biodegradable Polymer Blends of Poly(sebacic anhydride) and Poly(DL-lactic acid)

M. C. Davies,* K. M. Shakesheff, A. G. Shard, A. Domb,† C. J. Roberts, S. J. B. Tendler, and P. M. Williams

Laboratory of Biophysics and Surface Analysis, Department of Pharmaceutical Sciences, The University of Nottingham, Nottingham NG7 2RD, U.K.

Received June 23, 1995; Revised Manuscript Received November 27, 1995[⊗]

ABSTRACT: The erosion behavior of blends of biodegradable polymers is determined by the chemical composition and the molecular organization of the surface of the material. Providing a comprehensive characterization of polymer blend surfaces requires a multi-instrumental approach, as no individual surface analysis technique can ascertain both the chemical and morphological nature of surfaces. In this study we have characterized the surfaces of immiscible and miscible blends of the biodegradable polymers poly(sebacic anhydride) (PSA) and poly(DL-lactic acid) (PLA) using the surface techniques of static secondary ion mass spectrometry (SSIMS), X-ray photoelectron spectroscopy (XPS), and atomic force microscopy (AFM). SSIMS and XPS have recorded the surface enrichment of all of the blends with the PLA component. For the immiscible blends, differential charging within the XPS spectra also provides evidence of phase separation. AFM data have contrasted the surface morphologies of the immiscible and miscible blends, and the use of *in situ* AFM techniques has enabled the effect of blend morphology on surface erosion to be visualized. For the immiscible systems, clear phase separation morphologies can be observed and at certain blend compositions the rapid loss of the PSA from the films results in the exposure of the PLA morphology. However, as the PLA content is increased, the surface enrichment effect results in the degradation behavior of the blend being dominated by the slow degrading PLA surface layer. For the miscible systems, the *in situ* AFM studies visualized a disintegration of the whole blend film without the exposure of a PLA morphology, indicating that the hydrolysis of the PSA component rendered the whole film unstable. The use of SIMS, XPS, and AFM, while highlighting the complexity of polymer blend surfaces, can provide a rapid analysis of the physicochemical phenomena underlying the organization of these systems and therefore should facilitate the application of such systems as biomaterials.

Introduction

In the application of synthetic polymers as biomaterials there is a demand for biodegradable substances that are naturally removed from the body after a desired response has been elicited.[1,2] A wide variety of biodegradable polymers have been investigated as potential biomaterials, particularly in the field of controlled drug delivery[3−7] where there is a requirement for polymers that breakdown with predictable kinetics. Much research in this area has concentrated on altering degradation kinetics through chemical modification of the polymer structure. For example, the hydrolysis of polyanhydride devices can be slowed by increasing the hydrophobicity of the backbone structure.[3] This chemical modification strategy has led to the production of versatile copolymer systems which are composed of monomers with different degradation susceptibilities.[8] The degradation kinetics of these copolymers can be controlled through altering the proportions of each monomer in the polymer.

Another approach in the design of biodegradable polymer devices with controllable hydrolytic kinetics is the use of polymer blends.[9−11] Blending biodegradable polymers offers the potential to fabricate new polymeric materials whose erosion kinetics and fabrication characteristics can be modified by varying blend composition.[12−14]

Despite this progress problems exist in the use of polymer blends in biodegradable applications due to the increased complexity of these materials. A common cause of this complexity is the tendency for many pairs of polymers to be immiscible in one another.[9] This immiscibility causes the material to separate into two phases and leads to the kinetics of biodegradation being substantially influenced by the morphology of the individual polymer phases. Another factor in the complexity of the blends is the tendency for one of the polymers to be expressed at the surface in preference to the other. This surface enrichment is driven by surface energetics[15] and clearly has considerable implications in the design of degradable materials because the kinetics of hydrolysis of the surface-enriched component may dominate the degradation kinetics of the whole device.

(a) PSA

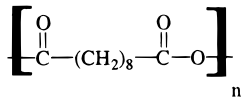

(b) PLA

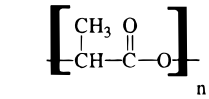

Figure 1. Chemical structures of (a) PSA and (b) PLA.

In this paper, we study a series of biodegradable polymer blends composed of poly(sebacic anhydride) (PSA) and poly(lactic acid) (PLA)[12] (Figure 1). Both of these polymers have been intensively investigated as potential biodegradable materials for use in drug delivery.[16−18] The PSA component is known to display a higher hydrolytic susceptibility in alkaline pH than the PLA component,[17] and therefore, it is anticipated that the overall degradation kinetics of the materials

† The Hebrew University of Jerusalem, School of Pharmacy, Jerusalem, Israel, 91120.

[⊗] Abstract published in *Advance ACS Abstracts,* February 15, 1996.

0024-9297/96/2229-2205$12.00/0

can be altered by varying the blend composition. It has been demonstrated that at relatively high molecular weights PSA and PLA are immiscible, but the polymers demonstrate some miscibility when the molecular weight of the PLA component is decreased to 3k and below.[12] In the present work we aim to examine the surface chemistry and morphology of the immiscible and miscible PSA/PLA blends with a view to understanding the influence of phase separation and surface enrichment on degradation.

Surface chemistry analysis has been performed by X-ray photoelectron spectroscopy (XPS) and static secondary ion mass spectrometry (SSIMS) to reveal any preferential surface segregation of blend components. These techniques probe the chemistry of the polymer surface to a depth of between 2 and 10 nm for XPS[19] and approximately 1 nm for SSIMS.[20] The use of both of these techniques to study the composition of biodegradable polymers and polymer blend surfaces is well established.[21−23] The analysis of the surface morphology of the polymer blends has been performed using an atomic force microscope (AFM).[24−27] This instrument allows the surfaces of the blend films to be imaged within an aqueous liquid environment, enabling structural three-dimensional data to be obtained. AFM analysis has been used to study the effect of blend composition on polymer phase morphology. *In situ* AFM studies have been performed to record changes occurring to the blend surfaces during hydrolytic degradation.

Experimental Section

Polymer Film Preparation. PSA (25k) was synthesized by melt polycondensation of sebacic acid.[28] PLA (50k and 2k) was used as obtained (Polysciences, Inc., Warrington, U.K.). Thin film samples were prepared by spin casting aliquots (20 μL) of polymer solutions (1% w/v in chloroform) onto a substrate. Blend film production was achieved by mixing solutions of the homopolymers in the desired proportions.

XPS Analysis. The XPS spectra were acquired using a Scienta ESCA300 electron spectrometer employing monochromated Al Kα (1486.7 eV) X-rays. This instrument has been described in detail elsewhere.[29,30] The X-ray gun was operated at 2.8 kW and the electron take-off angle to the spectrometer was 90° from the sample surface unless stated otherwise. This gives an approximate sampling depth of 9 nm for C 1s electrons.[19] Samples were spun cast onto argon ion sputter cleaned silicon wafers. In most cases the polymer blend films were thin enough to obviate the need for charge compensation. Survey spectra (0−1150 eV binding energy) were collected using a pass energy of 300 eV and a slit width of 1.9 mm. Narrow scans of the elemental core lines were taken with a pass energy of 150 eV and slit widths of 0.5 mm.

SSIMS Analysis. SSIMS spectra were collected using a VG Ionex SIMSLAB 3B instrument equipped with a differentially pumped EX05 ion gun and a 12-12M quadrupole mass spectrometer. The main chamber routinely achieves a base pressure of better than 10^{-9} mbar, and during operation this rises to approximately 10^{-7} mbar. The total dose per sample was less than 10^{13} atoms/cm^2, which is the threshold for the static SIMS regime.[31] Polymer samples were spun cast onto sample stubs coated with clean aluminum foil.

AFM Analysis. Atomic force microscopy was performed with a Topometrix TMX2000 Explorer (J. K. Instruments, Saffron Walden, Essex, U.K.). Topographies were obtained with Si_3N_4 probes on cantilevers with spring constants of 0.032 N/m (Park Scientific). All images were recorded with the sample, probe, and cantilever immersed in an aqueous solution. Initial surface characterization was performed in a water environment at pH 7. *In situ* AFM imaging of topographical changes occurring as the polymer films degrade was performed by exchanging the pH 7 water with a pH 12.4 NaOH(aq) solution. Images were then recorded at regular intervals. The AFM topographs presented in this paper are shown as shaded data in which the image is displayed as if illuminated at a shallow angle from the right hand side of the image. Samples were spun cast onto glass substrates.

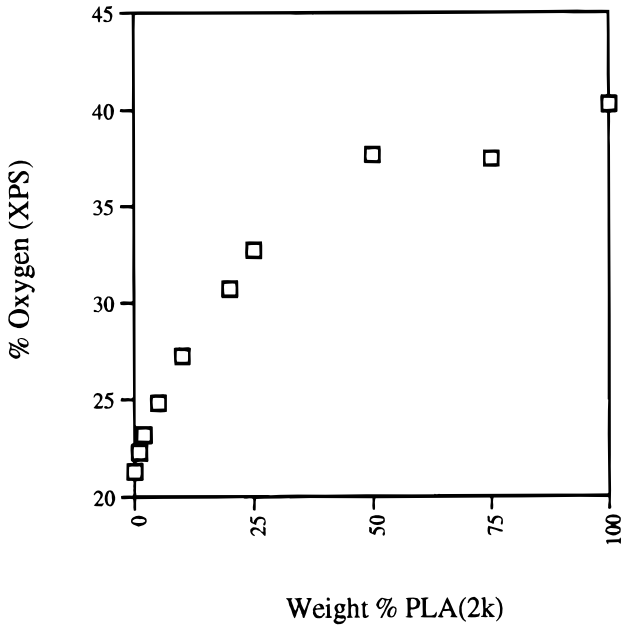

Figure 2. Comparison of surface oxygen with bulk weight % of PLA for PSA/PLA (2k) blends.

Results and Discussion

XPS Analysis. *Homopolymers.* Wide scans of all the blends demonstrate the presence of only two elements, carbon and oxygen. The absence of any signal from the silicon substrate suggests that the films are uniformly at least 10 nm thick. The C 1s and O 1s spectra of the pure PSA and PLA (2k) oligomer were in excellent agreement with previously published work.[32] The PLA (50k), however, showed a higher degree of sample charging (~2.5 eV) compared to the oligomer (~1 eV) and also wider peaks (C 1s FWHM PLA (50k) ~1.4 eV, PLA (2k) ~1.1 eV). It is apparent that the peak broadening is associated with sample charging since application of charge compensation from the electron flood gun reduced the half-width of the peaks to values comparable with that of the oligomer. This charging is indicative of a thicker film being formed in the case of the high molecular weight species. Since the concentrations of the solutions used to prepare the films are identical, and all other parameters in the sample preparation are constant, this effect may arise from the PLA (50k) solution having a larger viscosity than the oligomer,[33] causing the polymer to spread more slowly across the sample stub face during the spin-casting procedure, resulting in the formation of a thicker film.

Miscible PSA/PLA (2k) Blends. The PLA oligomer is known to be miscible with PSA.[12] Even though the two polymers will not segregate into domains within the bulk, it is possible that there will be preferential enrichment of one of the components at the blend surface. In these studies we are dealing with freshly solvent cast films, and so the resulting surface may not be the thermodynamically favored one, but a result of solvent effects.[34] A comparison of the experimentally determined surface oxygen concentration with the bulk weight percent of PLA is plotted in Figure 2. The nonlinearity of the graph indicates that there is an excess of the PLA oligomer at the surface of the blend.

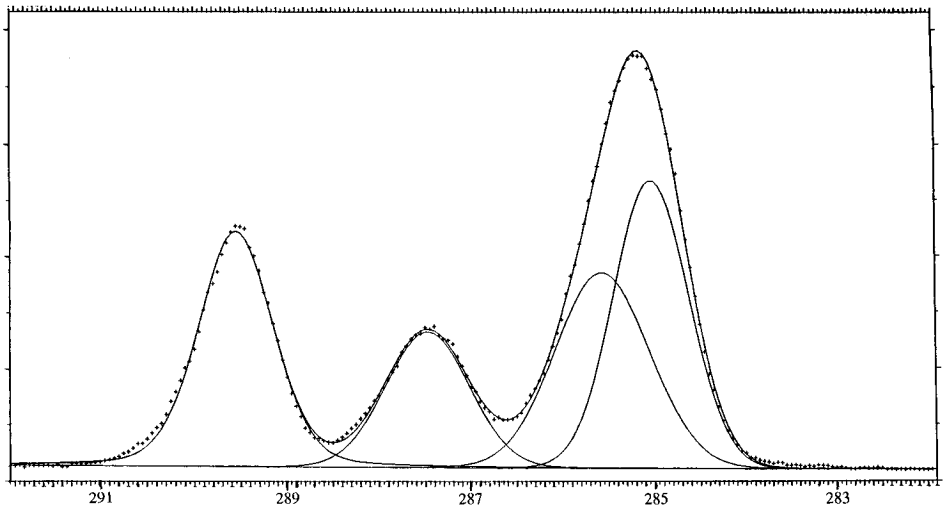

Figure 3. Peak-fitted C1s spectra for PSA/PLA (2k) blend, 25% PLA.

If the blend surface were identical to the bulk composition, one would expect a linear relationship between the oxygen concentration and the weight percent PLA.

An example of a peak-fitted C 1s spectra from one of the miscible blends is given in Figure 3. It was noted that the methyl group in PLA did not have the same binding energy as that of the methylene groups in PSA. A secondary shift of approximately 0.4 eV was found, presumably because of the close proximity of the electron deficient *C*—O atom, which itself is affected by the neighboring O=*C*—O group. We have found a similar secondary shift while analyzing block copolymers of PLA and poly(ethylene oxide).[35] Applying this observation to other peaks in the C 1s PLA spectrum results in the *C*—O peak appearing at ca. 287.4 eV and the O=*C*—O peak at ~289.45 eV, which is at almost exactly the same binding energy as the anhydride group in PSA. In the peak fits generally only four peaks were used; in order of increasing binding energy these represent the chemical groups CH_2 (PSA) = 285 eV, CH_3 (PLA) + CH_2COO (PSA) = 285.4−285.5 eV, *C*—O (PLA) = 287.4 eV, and O=*C*—O (PLA + PSA) = 289.45 eV. Only the third of these peaks contains a contribution solely from the PLA and does not significantly overlap any other peak. This peak was, therefore, used as a measure of the surface molar percent of the PLA repeat unit, and a comparison is made with the bulk value in Figure 4. Once again there is clear indication that there is a surface excess of PLA.

Immiscible PSA/PLA (50k) Blends. Figure 5 shows a plot of the percent of oxygen within the immiscible polymer blend against the blend bulk composition. Again, the PLA component is dominantly expressed at the surface. In this respect the immiscible blends appear to be little different from the miscible polymers. However, an examination of the high-resolution C 1s spectra reveals quite different features. Figure 6 shows the unfitted C 1s spectrum of the 50% PLA blend with and without charge compensation (using an electron flood gun). The charge-compensated spectrum is extremely similar to that of the miscible 50% PLA (2k) blend, but without charge compensation there appears to be a broadening of all peaks and shifting of the *C*—O and O=*C*—O peaks to higher binding energy. This effect was found in both the 50% and 25% PLA (50k) blends. Peak fitting the spectra which exhibited charging effects was possible with two sets of Gaussian peaks, each set constrained in relative area and relative

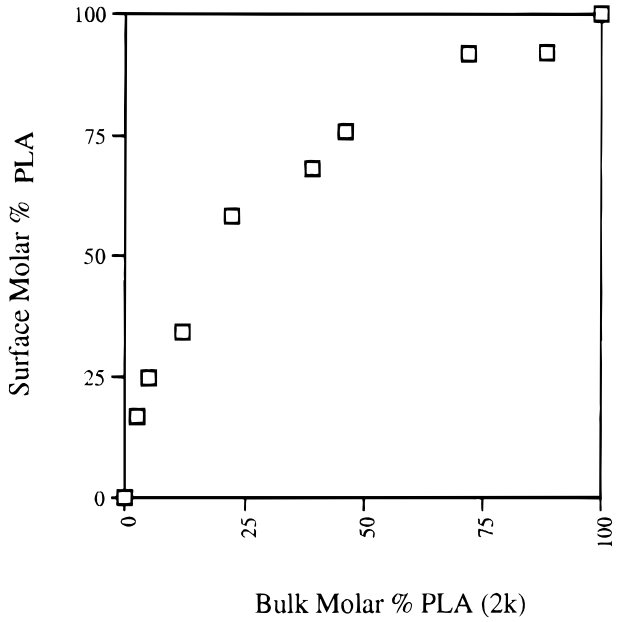

Figure 4. Surface molar % of PLA repeat unit determined from C 1s peak fitting against bulk molar % for PSA/PLA (2k) blend.

position to represent pure PLA and PSA components. It was found that good fits could be obtained if the PLA components were shifted by between 1 and 1.3 eV binding energy above those of the PSA. This difference in charging is similar to that found between the PLA (50k) and PLA (2k) homopolymer films and may once again be ascribed to a difference in film thickness leading to insufficient charge compensation from photoelectrons arising from the silicon substrate. The two components of the blend do not charge to the same degree, and this is almost certainly a product of the immiscible nature of the polymer blend. One would expect a miscible polymer to exhibit uniform charging in both components, since the two components are in intimate contact, but for this sample, there is an electrical isolation of the two different polymers, with the PLA rich domains exhibiting a higher positive charge than the PSA domains which may be explained most simply by the occurrence of phase separation within the blend surface.

SSIMS Analysis. *Homopolymers.* The spectra of both PSA and oligomeric PLA have been documented previously[36,37] and the films examined here showed no

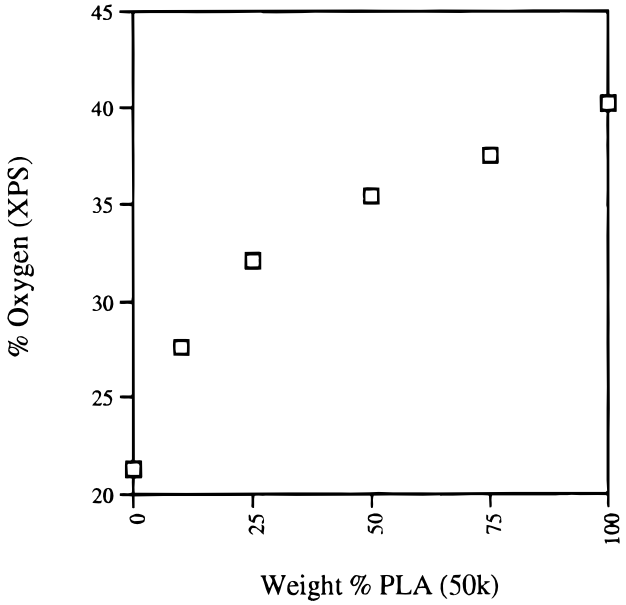

Figure 5. Comparison of surface oxygen with bulk weight % of PLA for PSA/PLA (2k) blends.

significant differences from these literature examples. The spectrum of PLA (50k) does show some significant differences in ion intensities from that of PLA (2k) and these are thought to derive from end-group effects.[38] The absence of a strong signal due to Al^+ at *m/z* 27 in all the samples indicates that polymer film thickness was greater than the sampling depth of the SSIMS experiment. None of the films, however, were thick enough to require the use of an electron flood gun to neutralize charging effects.

Miscible PSA/PLA (2k) Blends. All of the blends demonstrated the full range of ions associated with both PLA and PSA. No ions of mass numbers differing from those found in the homopolymers were noted. Figure 7 demonstrates an attempt to quantify the SSIMS data, where the intensity of an ion typical of PLA (*m/z* 200, $[3M - O]^{\bullet +}$)[36] is compared with an ion typical of PSA (*m/z* 185, $[MH]^+$).[37] Both of these ions are unique to the respective homopolymer and sufficiently close in mass to minimize mass dependent sensitivity changes. Furthermore, in the homopolymer spectra they are of comparable absolute intensities, and the value $I(200)/[I(200) + I(185)]$ can be at least qualitatively used as a measure of the surface concentration of PLA.[12] The curve shown in Figure 7 demonstrates features similar to those of the XPS data, with a surface excess of PLA being exhibited in all of the blends.

Immiscible PSA/PLA (50k) Blends. A similar plot of ion intensity against bulk PLA weight % is given in Figure 8. Once again, this shows broad agreement with both the miscible blends and XPS data. The presence of an ion signal for PSA in all of the polymer blends perhaps indicates that there is an extension of the PSA domains to the top ~1 nm of the surface even when there is a large excess of the surface active PLA. This result may also be explained, however, by a small, but detectable, concentration of PSA being present in the PLA domains. There is no significant difference between these immiscible blends and the miscible PLA (2k) systems. XPS investigations revealed substantial charging differences between the two phases of polymer in the PSA/PLA (50k) mixtures; however, no charging was apparent during the SSIMS investigations. If they did occur, we could expect differences in the energy distributions of ions arising from each of the phases, and thus because of the energy dependency of quadrupole mass spectrometers,[20] these effects should be obvious. In this case it appears that X-ray excitation is more prone to produce differential charging than atom bombardment.

AFM Analysis. *Immiscible PSA/PLA (50k) Blends.* The thin films of PSA and PLA (50k) and the blends containing differing proportions of these two polymers displayed distinct surface morphologies when analyzed with the AFM. The film produced from the PSA solution possessed spherulites at the surface. The AFM topograph in Figure 9a shows a typical 10 μm × 10 μm area of the PSA film. The spherulites can be identified by the fibrous structures radiating from nucleating centers. During the growth of the spherulites in the film solidification, the fibers grow out from the nucleating centers and fill space in two dimensions. As this growth continues, the fibers from neighboring developing spherulites impinge on each other and grain boundaries form.[39] The presence of spherulitic structures in the surface topography of the PSA film is indicative of the semicrystalline nature of this homopolymer.[40] The fibers are formed from crystalline lamellar structures. However, there is also amorphous polymer material present in the film between the crystalline lamellae and the fibers.

The surface topography of the single component PLA films was found to be relatively smooth and lacking in the spherulitic structures commonly observed by the AFM for more crystalline polymers.[41] In Figure 9e, the surface topography of a 10 μm × 10 μm area of a PLA film is shown. This image shows a smooth film structure disrupted only by occasional aggregates. This type of surface morphology is typical of a low-crystallinity polymer sample prepared by spin casting.

For the polymer blend containing 70% PSA:30% PLA, the surface was observed to consist of a granular morphology (Figure 9b). The granules had diameters ranging from 200 nm to 1 μm and protruded from the other surface material by 10−50 nm. Between the granules, the polymer film appears to be continuous.

When the polymer blend composition is changed to 50% PSA:50% PLA, the AFM-recorded topography changes to show a gently pitted surface. This surface morphology can be observed in the AFM topograph in Figure 9c. The pits have a broad and shallow structure with typical diameters ranging from 400 nm to 2 μm and depths of 20−60 nm.

A pitted surface morphology was also observed for the film of the 30% PSA:70% PLA blend (Figure 9d). However, the AFM images showed the pits to be smaller in diameter than the 50% PSA:50% PLA blend film. The diameter of these pits was found to be between 200 and 800 nm with depths between 20 and 50 nm.

For all the polymer blends studied it is evident that the presence of PLA has inhibited the formation of identifiable fibrous structures by the PSA component. Even at a high relative PSA composition of 70%, the crystallization process appears to have been significantly impaired.

We have previously shown that *in situ* AFM studies, performed within an aqueous environment can visualize the dynamic morphological changes occurring as polymer films are degraded.[42,43] In these studies the AFM is imaging the biodegradable polymer at the interface between the polymer surface and the hydrolyzing medium. Using this technique, we have observed the

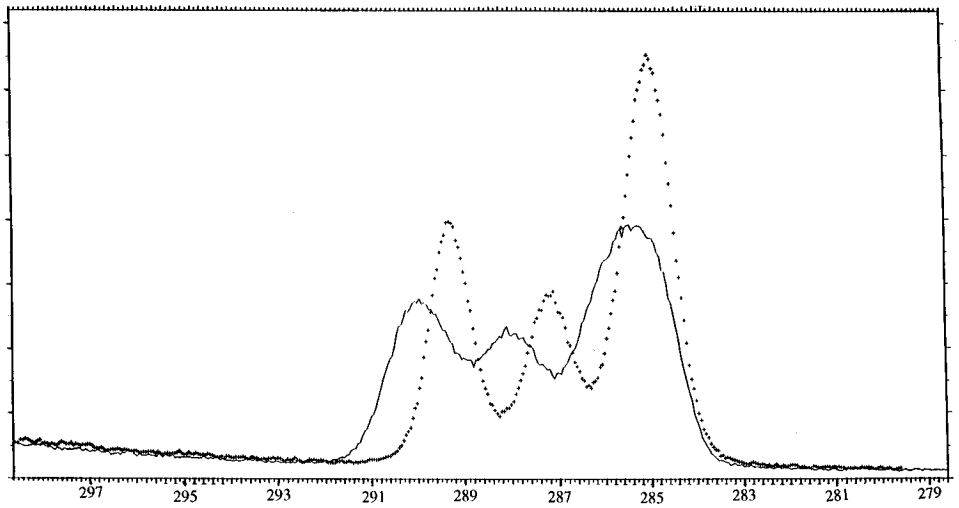

Figure 6. C1s spectrum of 50% PLA blend with (crosses) and without (solid line) electron flood gun on.

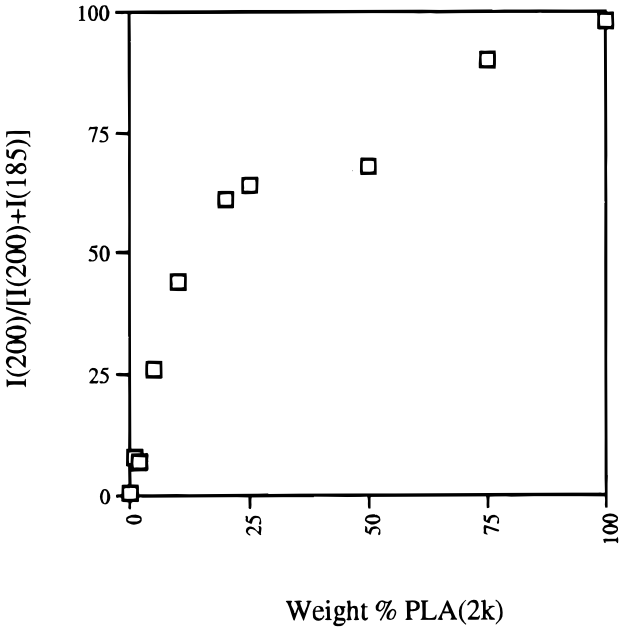

Figure 7. Quantification of SIMS PSA/PLA (2k) data.

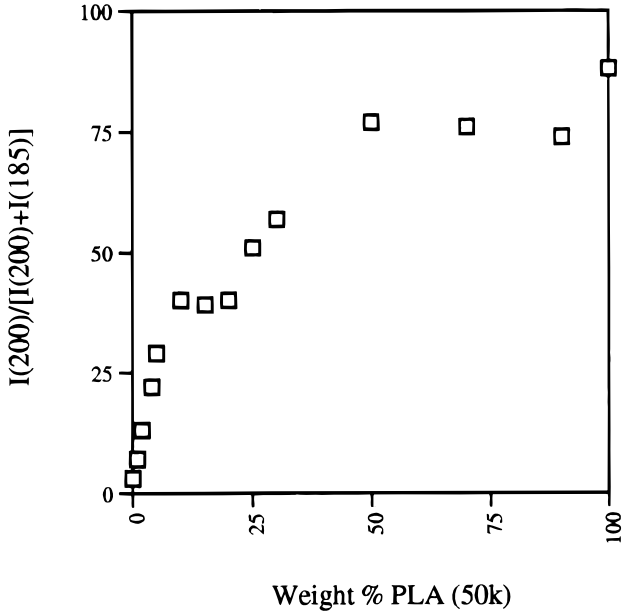

Figure 8. Quantification of SIMS PSA/PLA (50k) data.

surface morphology changes of solvent-cast and melt-crystallized PSA films. It was found that the AFM could visualize the preferential loss of amorphous PSA material from spherulites. This loss occurs due to higher permeability of the amorphous material compared to the crystalline fibers,[40] resulting in a higher proportion of potential hydrolysis sites and hence a higher probability of random chain scission.

The two polymers in these blends are known to erode at very different rates in aqueous environments.[44] In physiological conditions, the PSA is eliminated from the body within 2−4 weeks, while the PLA is eliminated within 12−16 weeks. Therefore, initial changes in surface morphology should be caused by the loss of the PSA material in the films and the morphology of the PLA material should be exposed. On the basis of the above elimination times, the *in situ* AFM experiments were performed at pH 12.5. At this pH the hydrolysis of both polymers is catalyzed, enabling the erosion of each blend to be studied over relatively short time periods. The experiments described here could equally be performed at physiological pH values.

For 70% PSA:30% PLA films the initial granular continuous film structure observed in the original film

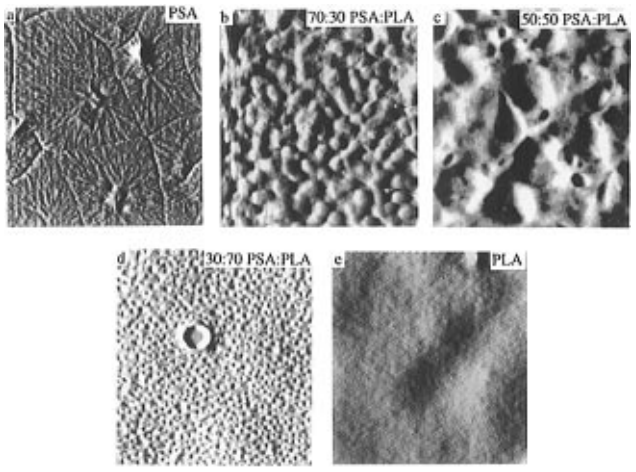

Figure 9. 10 μm × 10 μm AFM images of the surface topography of PSA and PLA (50k) in single component and blended thin films.

was rapidly changed in the degradation experiment. The four 10 μm × 10 μm AFM images in Figure 10 show data recorded at degradation times of 0, 2, 5, and 10 min. These images show that the granular features

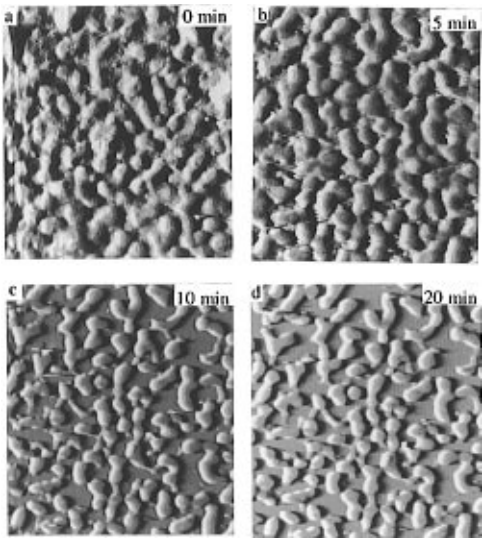

Figure 10. *In situ* AFM images of the degradation of a 70% PSA:30% PLA (50k) blend. Image dimensions: 10 μm × 10 μm.

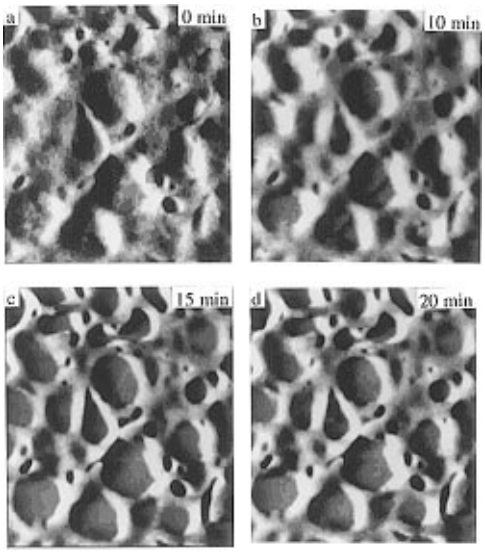

Figure 11. *In situ* AFM images of the degradation of a 50% PSA:50% PLA (50k) blend. Image dimensions: 10 μm × 10 μm.

remain relatively constant in the first stages of erosion, while the polymer material between the granules is lost at a more rapid rate. In the image taken following 5 min of degradation the granules are more distinct from the rest of the film. This process continues until after 10 min of degradation the granules remain as isolated islands on the substrate surface. These data indicate that the PLA material is present as granules in the initial film. PSA material is found between the PLA granules prior to the erosion to give the continuous film observed in the initial surface morphology studies.

In Figure 11, four 10 μm × 10 μm AFM images are displayed which show the erosion of the 50% PSA:50% PLA blend film. Surface topographs prior to the degradation showed a continuous film with broad, shallow pits in the surface. As the degradation proceeds, these pits can be observed to broaden and deepen. As this erosion process continues, a network structure is exposed. This network structure remained on the surface for over 40 min of exposure to the pH 12.5 NaOH aqueous solution.

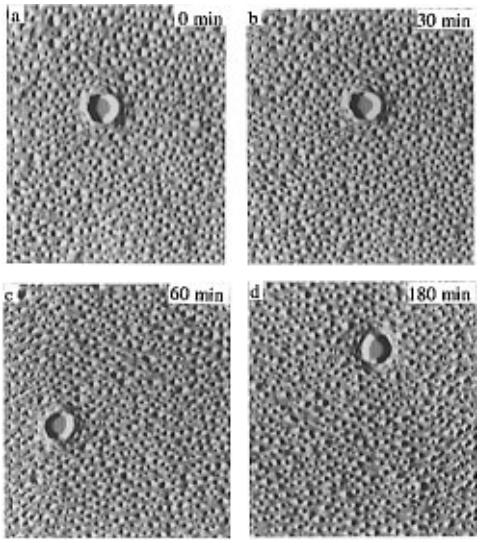

Figure 12. *In situ* AFM images of the degradation of a 30% PSA:70% PLA (50k) blend. Image dimensions: 10 μm × 10 μm.

Thus for the 50% PSA:50% PLA film, the erosion and loss of PSA material results in the exposure of a network of PLA. Here, the degradation experiment has revealed a fundamental difference in film morphology between the 70% PSA:30%PLA film and the 50% PSA:50% PLA film. As the amount of PLA in the blend is increased, an inversion in the phase morphology occurs with the PLA morphology changing from isolated granules in a network of PSA to a network of PLA separating areas of PSA. The AFM-recorded phase separations support the theory of differential charging resulting from the two insulating phases, as observed by XPS.

Further increasing the proportion of PLA in the blend had a dramatic effect on the degradation characteristics of the thin films. The AFM data recorded during the erosion of the 30% PSA:70% PLA is shown in Figure 12. The most noticeable feature of this series of images is the time scale over which they were taken. The final image was recorded 3 h after the first exposure of the blend to pH 12.5, demonstrating the resistance of the blend to degradation, the other blends showed clear erosion within 10 min, and the films became unstable within 40 min. The only evidence of degradation occurring to the 30% PSA:70% PLA film is a slight increase in the depth of the pits during the first 30 min of the experiment.

Clearly, this blend is displaying a pattern of degradation very different from those of the blends with lower PLA concentrations. It appears that the surface enrichment of PLA, which was detected by XPS analysis, has produced a barrier between the PSA and the pH 12.5 solution. Hence, the kinetics of degradation are determined by the slowly degrading PLA only. For the lower PLA content blend films, there appears to be insufficient surface PLA material to prevent permeation of the hydrolyzing solution to the PSA material and hence the film becomes unstable to the high-pH environment within minutes of exposure.

Miscible PSA/PLA (2k) Blends. AFM images of the films produced from PLA (2k) and PSA are shown in Figure 13. The PLA (2k) film shown in Figure 13e displayed a smooth surface topography similar to that of the PLA (50k). When the PSA and PLA (2k) were blended, the resulting films all displayed particulate

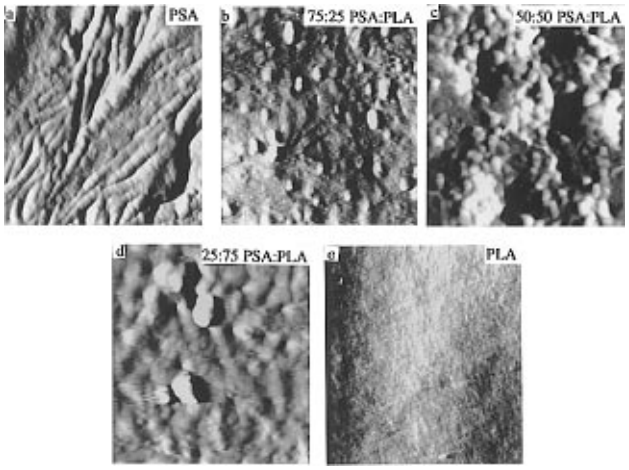

Figure 13. AFM images of the surface topography of PSA and PLA (2k) in single component and blended thin films. Image dimensions: 3 μm × 3 μm.

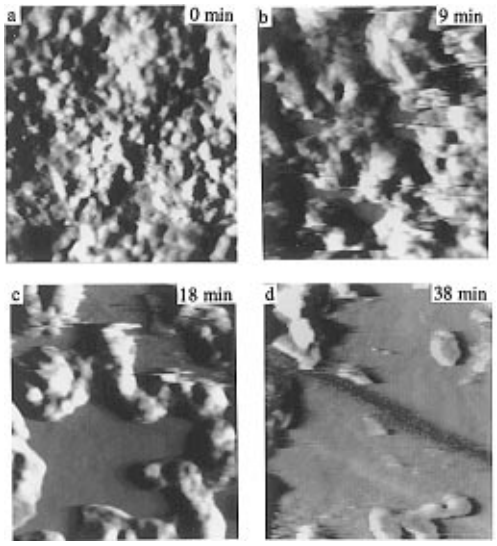

Figure 14. *In situ* AFM images of the degradation of a 50% PSA:50% PLA (2k) blend. Image dimensions: 10 μm × 10 μm.

surface morphologies which were very different from the surfaces of the PSA only and PLA only films. An AFM image of the 70% PSA:30% PLA film is shown in Figure 13b. There is no evidence of fibrous features due to the semicrystalline PSA, indicating that the PLA (2k) has inhibited the crystallization process; instead the film is composed of particles with diameters ranging from 40 to 300 nm. As the relative proportion of PLA (2k) is increased, the surface topographies recorded by the AFM continue to display a particulate surface structure.

The surface topographies of the partially miscible PSA:PLA (2k) films are clearly different from the recorded topographies of the immiscible PSA:PLA (50k) films. However, the real difference in the organization of the polymeric materials in these films is revealed by the *in situ* AFM imaging of the degradation. The series of AFM images in Figure 14 were recorded during the degradation of a 50% PSA:50% PLA (2k) film in a pH 12.4 aqueous solution. The images show the removal of the polymeric film and the exposure of the smooth glass substrate. Clear surface topography changes can be observed in the first 10 min of contact with the pH 12.4 aqueous solution. The particulate structure of the film surface becomes less distinct at this stage, and there is some evidence of the AFM damaging the film as it scans, indicating a softening of the surface material. After 9 min of contact with the hydrolyzing environment, the glass substrate becomes exposed and then over the next 29 min, there is a gradual removal of the remaining polymer material. It is noticeable that the degradation process does not result in the exposure of an underlying PLA morphology. This finding is consistent with the PSA and PLA being mixed on a nanometer scale in the partially miscible blend. Hence, as the PSA material is degraded, the film structure becomes unstable. This results in the loss of the film as a whole over the 60 min period, rather than the pattern observed for the immiscible blends in which the PSA material is lost rapidly, leaving the PLA material on the substrate.

Conclusions

Surface analysis of the PSA/PLA blends has detected both phase separation and surface enrichment. XPS and SSIMS reveal that in all the systems investigated, whatever the bulk concentrations or whether the polymers are miscible or immiscible, there is a surface excess of PLA. In the case of the immiscible PSA/PLA (50k) blends evidence was provided for phase separation by the occurrence of differential charging between the two phases. This charging phenomenon did not occur for the miscible PSA/PLA (2k) blends, and although this is not conclusive evidence for miscibility, there is a concordance between the XPS data and AFM data on these two mixtures. Despite the strong surface excess of PLA, the presence of PSA in all of the blends may be detected by the presence of diagnostic ions in the SSIMS spectra. Whether this is due to phase-separated PSA being present in the top surface layer or to there being a low concentration of PSA present in the PLA phase is unknown.

These findings are in accord with the atomic force microscopy studies, which emphasize the importance of phase separation and surface enrichment on the degradation of the polymer films. For the PSA/PLA (50k) blends, the phase separations become apparent when the changes in surface morphology are imaged during degradation. For the 70%:30% and 50%:50% PSA/PLA (50k) blends the hydrolyzing medium rapidly attacks the PSA phase, resulting in the exposure of the PLA morphology. However, the 30%:70% PSA/PLA (50k) blend displays a very slow surface erosion, indicating that the surface enrichment of the PLA dominates the degradation behavior of the film. Particulate surface morphologies were observed for the PSA/PLA (2k) miscible films, and on degradation, the *in situ* AFM images recorded a general disintegration of the film.

By combining the surface chemical information of SSIMS and XPS data with the surface morphology of the AFM data, it is possible to characterize the complex surfaces of biodegradable polymer blends and record the effect of the surface organization on degradation. The effects of both phase separation and surface enrichment in such blends is contributing to our understanding of the bulk and surface chemistry and morphology, information which has important implications for the design of new biodegradable materials.

Acknowledgment. The authors would like to acknowledge the support of the BRITE/Euram program, the ESPRC/DTI Nanotechnology LINK program, VG Microtech, Kodak Limited, and Oxford Molecular Group plc. Many thanks to Graham Beamson at Rusti, Daresbury Laboratory, U.K., for collecting the XPS spectra.

References and Notes

(1) Langer, R. *Science* **1990**, *249*, 1527−1533.
(2) Langer, R.; Vacanti, J. P. *Science* **1993**, *260*, 920−926.
(3) Tamada, J.; Langer, R. *J. Biomater. Sci., Polym. Ed.* **1992**, *3*, 315.
(4) Davis, S. S. *J. Pharm. Pharmacol.* **1992**, *S1*, 186−190.
(5) Heller, J. *J. Controlled Release* **1985**, *2*, 167.
(6) Leong, K. W.; Langer, R. *Adv. Drug Delivery Rev.* **1987**, *1*, 199.
(7) Heller, J. *Adv. Drug Delivery Rev.* **1993**, *10*, 163−204.
(8) Leong, K. W.; Brott, B. C.; Langer, R. *J. Biomed. Mater. Res.* **1985**, *19*, 941.
(9) Paul, D. R., Newman, S., Eds. In *Polymer Blends*; Academic Press: New York, 1979; Vol. 2.
(10) Paul, D. R.; Barlow, J. N.; Keskkula, H. In *Encyclopedia of Polymer Science and Engineering*; Krowschwitz, J. I., Ed.; John Wiley & Sons: New York, 1988.
(11) Woodward, A. E. *Atlas of Polymer Morphology*; Hanser Publishers and Oxford University Press: Munich and Oxford, 1989; Chapter 9.
(12) Domb, A. J. *J. Polym. Sci., Part A: Polym. Chem.* **1993**, *31*, 1973.
(13) Park, T. G.; Cohen, S.; Langer, R. *Macromolecules* **1992**, *25*, 116.
(14) Kumagai, Y.; Doi, Y. *Sumitomo Search* **1993**, *52*, 155.
(15) Jones, R. A. L.; Kramer, E. J.; Rafailovich, M. H.; Sokolov, J.; Schwarz, S. A. *Phys. Rev. Lett.* **1989**, *62*, 280.
(16) Göpferich, A.; Langer, R. *J. Polym. Sci.* **1993**, *31*, 2445.
(17) Domb, A. J.; Amselem, S.; Maniar, M. In *Polymeric Biomaterials*; Dumitriu, Ed.; Marcel Dekker, Inc.: New York, 1994; Chapter 13.
(18) Chasin, M.; Domb, A.; Ron, E.; Mathiowitz, E.; Leong, K.; Laurencin, C.; Brem, H.; Grossman, S.; Langer, R. In *Biodegradable Polymers as Drug Delivery Systems*; Chasin, M., Langer, R., Eds.; Marcel Dekker, Inc.: New York, 1990.
(19) Lukas, J.; Jezek, B. *Collect. Czech. Chem. Commun.* **1983**, *48*, 2909.
(20) Briggs, D. In *Ion and Neutral Spectroscopy*; Briggs, D., Seah, M. P., Eds.; Practical Surface Analysis; Wiley: Chichester, 1992; Vol. 2.
(21) Clark, D. T. in *Handbook of X-ray and Ultraviolet Spectroscopy*; Briggs D., Ed.; Heydon and Son Ltd.: London, 1977.
(22) Thomas, H. R.; O'Malley, J. J. *Macromolecules* **1981**, *14*, 1316.
(23) Thompson, P. M. *Anal. Chem.* **1991**, *63*, 2447.
(24) Roberts, C. J.; Williams, P. M.; Davies, M. C.; Jackson, D. E.; Tendler, S. J. B. *Trends Biotechnol.* **1994**, *12*, 127.
(25) Leggett, G. L.; Davies, M. C.; Jackson, D. E.; Roberts, C. J.; Tendler, S. J. B. *Trends Polym. Sci.* **1993**, *1*, 115.
(26) Drake, B.; Prater, C. B.; Weisenhorn, A. L.; Gould, S. A. C.; Albrecht, T. R.; Quate, C. F.; Cannell, D. S.; Hansma, H. G.; Hansma, P. K. *Science* **1989**, *243*, 1586.
(27) Marti, O.; Ribi, H. O.; Drake, B.; Albrecht, T. R.; Quate, C. F.; Hansma, P. K. *Science* **1988**, *239*, 50−53.
(28) Domb, A. J.; Langer R. *J. Polym. Sci., Part A: Chem. Ed.* **1991**, *42*, 1597.
(29) Beamson, G.; Briggs, D.; Davies, S. F.; Fletcher, I. W.; Clark, D. T.; Howard, J.; Gelius, U.; Wannberg, B.; Balzer P. *Surf. Interface Anal.* **1990**, *15*, 541.
(30) Gelius, U.; Wannberg, B.; Baltzer, P.; Fellner-Feldegg, H.; Carlsson, G.; Johansson, C.-G.; Larsson, J.; Münger, P.; Vegerfors, G. *J. Electron Spectrosc. Relat. Phenom.* **1990**, *52*, 747.
(31) Briggs, D.; Hearn, M. J. *Vacuum* **1986**, *36*, 1005.
(32) Beamson, G.; Briggs, D. In *High Resolution XPS of Organic Polymers*; Wiley: Chichester, U. K., 1992.
(33) *Polymer Handbook*; Brandrup, J., Immergut, E. H., Eds.; Wiley: New York, 1966.
(34) Garbassi, F.; Morra, M.; Occhiello, E. In *Polymer Surfaces, from Physics to Technology*; Wiley: Chichester, U. K., 1994; p 275.
(35) Shard, A. G.; Volland, C.; Li, Y.; Davies, M. C.; Kissel, T. *Macromolecules*, submitted.
(36) Davies, M. C.; Short, R. D.; Khan, M. A.; Watts, J. F.; Brown, A.; Eccles, A. J.; Humphrey, P.; Vickerman, J. C.; Vert, M. *Surf. Interface Anal.* **1989**, *14*, 115.
(37) Davies, M. C.; Khan, M. A.; Domb, A.; Langer, R.; Watts, J. F.; Paul, A. J. *J. Appl. Polym. Sci.* **1991**, *42*, 1597.
(38) Shard, A. G.; Volland, C.; Davies, M. C.; Kissel, T. *Macromolecules*, in press.
(39) Bassett, D. C. *CRC Crit. Rev. Solid State Mater. Sci.* **1984**, *12*, 97.
(40) Mathiowitz, E.; Jacob, J.; Pekarek, K.; Chickering D. *Macromolecules* **1993**, *26*, 5915.
(41) Shakesheff, K. M.; Davies, M. C.; Jackson, D. E.; Leggett, G. J.; Roberts, C. J.; Tendler, S. J. B.; Williams, P. M. *Nanobiology* **1994**, *3*, 41.
(42) Shakesheff, K. M.; Davies, M. C.; Roberts, C. J.; Tendler, S. J. B.; Shard, A.; Domb, A. *Langmuir* **1994**, *10*, 4417.
(43) Shakesheff, K. M.; Davies, M. C.; Domb, A.; Roberts, C. J.; Tendler, S. J. B.; Williams, P. M. *Macromolecules* **1995**, *28*, 1108.
(44) Domb, A. J. In *Polymeric Site-Specific Pharmacotherapy*; Domb, A. J., Ed.; John Wiley & Sons: Chichester, U.K., 1993; Chapter 1.

MA950889H